Numerical Calculation of the Characteristics of an Isolated AC Gas Discharge Display Panel Cell

Abstract: Device characteristics calculated from a one-dimensional dynamic simulation, incorporating space charge effects, of the gaseous discharge occurring at an isolated cell of an ac gas discharge panel are presented. The theoretical model shows all the qualitative features associated with plasma panels, and the quantitative agreement with experimental data inspires confidence in the general validity of the method.

Introduction

This paper describes briefly the device characteristics calculated from a one-dimensional numerical simulation of the dynamics of the electrical discharge occurring at an isolated site in an ac gas display panel [1]. Earlier attempts [2–5] to model the behavior of individual panel cells have been reviewed by Weber [6]. The salient features in the evolution of our modeling effort have also been briefly summarized [7]. The present analysis involves a self-consistent simultaneous solution of Poisson's equation, the transport equations, and the continuity equations for five particle species.

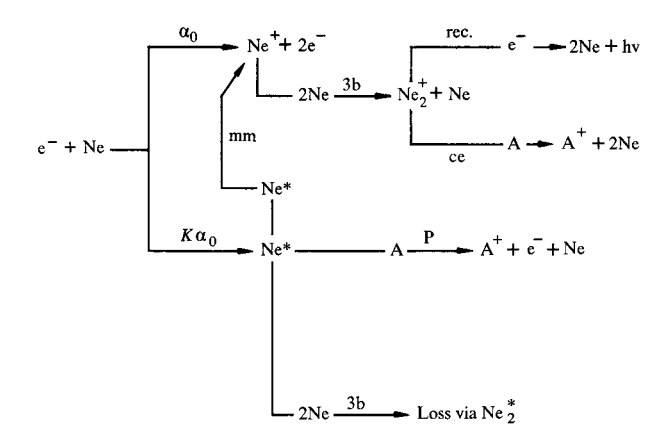
The model

Figure 1 shows schematically the various volume reactions included in the analysis. The symbol α_0 on this diagram represents Townsend's first coefficient for pure neon, which is a strong function of E/P. Values of α_n (E/P) were measured by others [8] under relatively low pressure and dc conditions. The quantity K is the number of metastable neon atoms generated per neon ion. This ratio is also a function of E/P and was deduced [9] from the measured values of α for both pure neon and the appropriate neon-argon mixture. The reaction rate for the collisional chemi-ionization of argon atoms by the neon metastable atoms was taken [10] to be 10^{-10} cm³-s⁻¹; the metastable-metastable ionization rate was estimated [11] to be 10^{-9} cm³-s⁻¹; the three-body deactivation rate for the neon metastable states has been measured [12] to be 5×10^{-34} cm⁶-s⁻¹; the three-body reaction rate for the conversion of an atomic neon ion to a molecular ion is

given [13] to be 4.4×10^{-32} cm⁶-s⁻¹; the rate of charge exchange from the molecular neon ion to the argon atom was taken [14] to be 5×10^{-14} cm³-s⁻¹; and the dissociative recombination coefficient for the molecular neon ion has been measured [15] to be 2.2×10^{-7} cm³-s⁻¹.

The model includes the back-scattering to the cathode of the secondary emitted electrons as a function of the ratio of the electric field at the cathode to the gas pressure [16, 17]. In addition, allowance was made for different

Figure 1 Schematic diagram of various volume reactions included in the analysis. The notations 3b, P, rec., mm, and ce represent 3-body interactions, collisional chemi-ionizations, electron-ion recombinations, metastable-metastable ionizations, and charge exchange reactions, respectively.



Copyright 1978 by International Business Machines Corporation. Copying is permitted without payment of royalty provided that (1) each reproduction is done without alteration and (2) the *Journal* reference and IBM copyright notice are included on the first page. The title and abstract may be used without further permission in computer-based and other information-service systems. Permission to *republish* other excerpts should be obtained from the Editor.

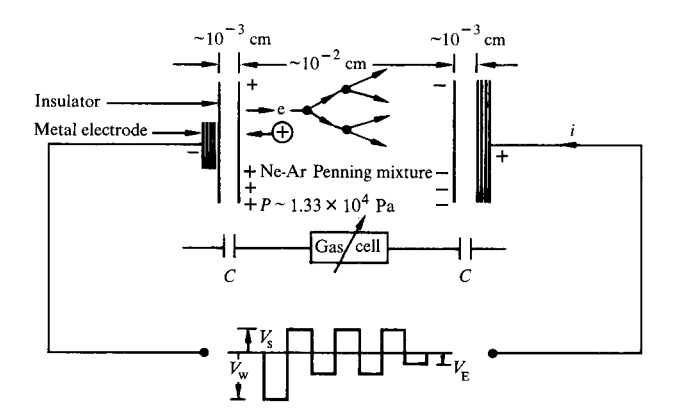


Figure 2 Physical arrangement and dimensions of panel.

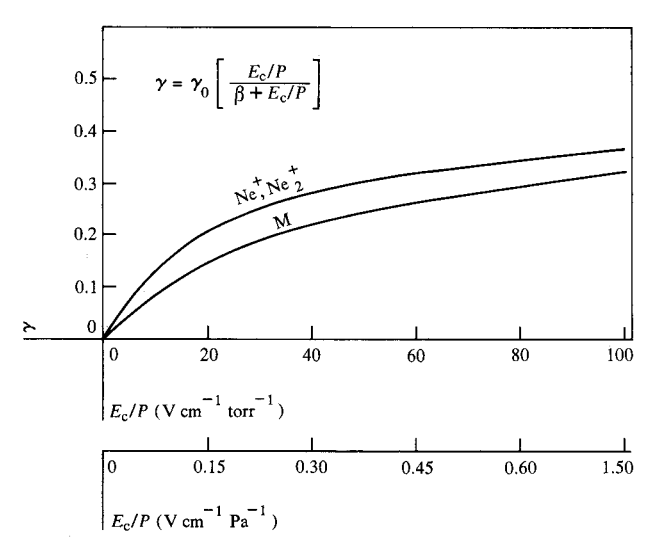


Figure 3 Effective coefficient of secondary-electron emission, γ , versus the reduced electric field, E_c/P , at the cathode. The top curve for the neon ions is for β =24, while the lower curve (neon metastables) is calculated for β =42. Both curves have γ_0 =0.45. (β is a function of initial average energy of emitted electrons.)

secondary-electron emission coefficients, in keeping with the difference in stored potential energy of the various species arriving at the cathode. An empirical correction procedure was invoked in the one-dimensional analysis to account for the dynamic lateral spreading of the active discharge area as a function of the current. The instantaneous current density was allowed to increase up to a fixed upper limit, beyond which the area of the discharge was increased dynamically to accommodate any further increase in the instantaneous value of the total current while keeping the current density fixed (this assumption is characteristic of the normal glow discharge region). The wall capacitance was also changed dynamically in consonance with the discharge area. The upper limit on the current density was adjusted to 0.31 A-cm⁻² in the pres-

ent work to fit the experimentally determined data on the instantaneous current peak. In addition to accounting for the dynamic spreading of the discharge, a practical necessity for the above correction procedure lies in its ability to prevent the instantaneous buildup of current density to very high transient values which lie beyond the handling capability of the numerical method. A comprehensive model [18] which includes both the metastable and the resonant radiation levels of neon does not require this artificial constraint on instantaneous current density. However, the computer time necessary to run this complete model is prohibitive for the numerous simulations required to match the experimental data.

Figure 2 shows the physical arrangement and dimensions of the panel and its electrical equivalent. Two thin glass insulators isolate the enclosed gas mixture (neon + 0.1 percent argon in this case) from orthogonal metal line electrodes. The cell is driven with square waves generated by a sustaining voltage source. The amplitude of the drive voltage can be modulated to produce $V_{\rm s}$, $V_{\rm w}$, and $V_{\rm e}$, which are the sustain, write, and erase signals, respectively.

The electric field in the gas imparts energy to the electrons which make ionizing and exciting collisions with neon atoms. The electrons continue to drift toward the anode, creating other collisions on the way. The ions drift (and the neon metastable atoms diffuse) to the cathode and produce secondary electrons. Upon emission from the cathode, some of these electrons are back-scattered to the cathode by collisions with the high pressure gas. As shown in Fig. 3, the back-scattering is a function of the initial average energy of the emitted electrons and the ratio of the electric field intensity at the cathode to the gas pressure [19]. The dynamic buildup of charge at the insulated electrodes results in a time-dependent voltage across the gas. The effective coefficient of secondary emission (γ) is, therefore, a function of time.

A novel algorithm [3], which used different time scales [5] for the transport of electrons and positive ions, was used to reduce the considerable computer time inherently required for this problem. The high ratio of electron to ion mobility was accommodated by dynamically partitioning the gas gap into regions of high and low electric field. In the high-field region near the cathode, the electrons were allowed to drift (and undergo avalanche ionization) for a time increment dictated essentially by the ion velocity adjacent to the cathode. Immediately following this region is the low-field region where the continuity equations were solved for both electrons and ions by subdividing the above time step into smaller time increments, which are short enough to keep a full account of the electrons.

Both the experimental and calculated results are for 466 \times 10² Pa of Ne + 0.1 percent Ar gas mixture in an approximately square cell area of 2.25×10^{-6} cm² (i.e., 0.15 mm

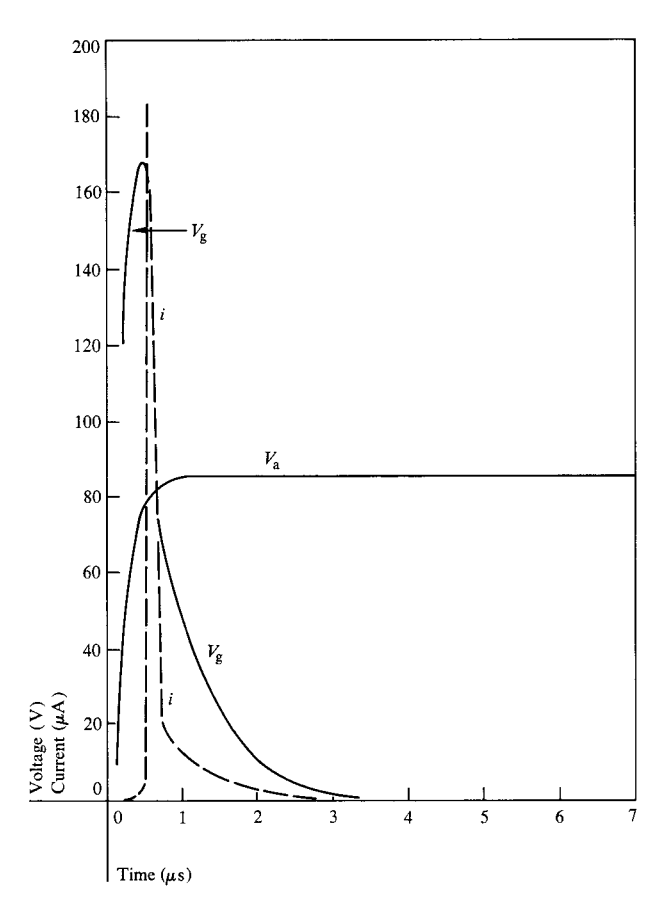
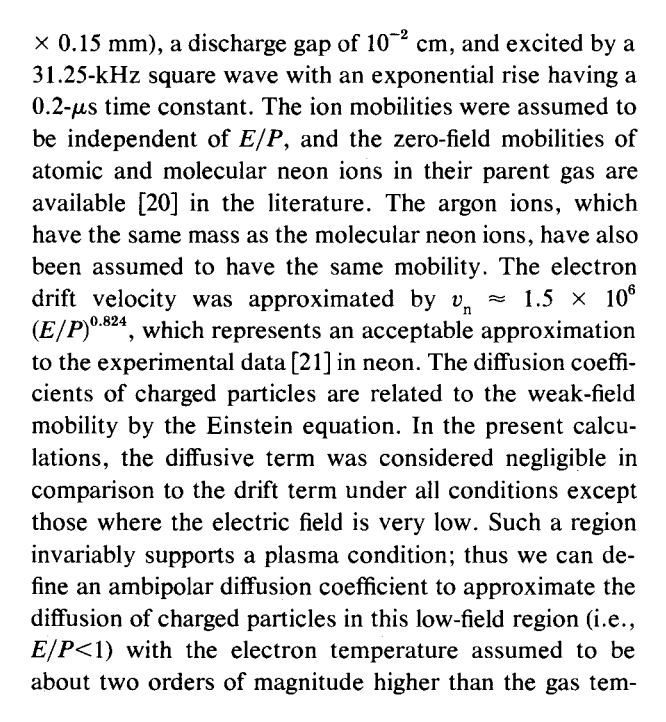


Figure 4 Applied voltage, $V_{\rm a}$, voltage across the gas, $V_{\rm g}$, and current, i, as functions of time.



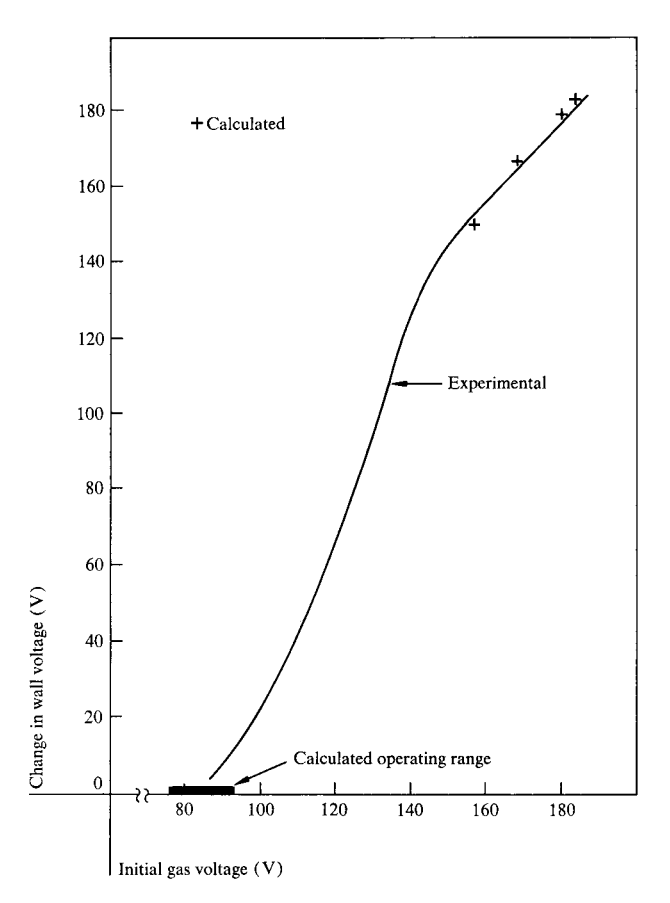
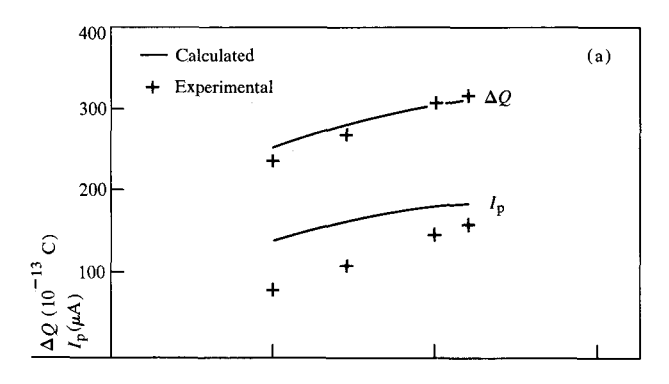


Figure 5 Comparison of experimentally determined voltage transfer curve with values computed by the theoretical model in the stable mode of operation.

perature. For the neutral metastable species of neon, the measured value of the diffusion coefficient in the parent gas is available [12].

The computation assumes a γ_0 for the neon and the argon ions; their specific values are determined by using them as the adjustable parameters to give a good fit between the calculated and the experimental results. The exact choice of γ_0 for the neon metastables is not critical, and it is chosen to be the same as that for neon ions. Estimates for the average speed of the emitted electrons are available for the neon ions, argon ions, and neon metastables [16]. Note that for simplicity, the atomic and molecular neon ions were assumed to behave identically. The results shown in Figs. 4–8 were calculated for a γ_0 of 0.45 for the neon ions and a γ_0 of 0.03 for the argon ions. These fitted values of γ_0 are in excellent agreement with recent measurements [22].

The wall capacitance per unit area (i.e., the ratio, per unit area, of the charge transfer to the voltage transfer) is adjusted to match the experimentally determined transfer of wall charge. The calculations reported here were done



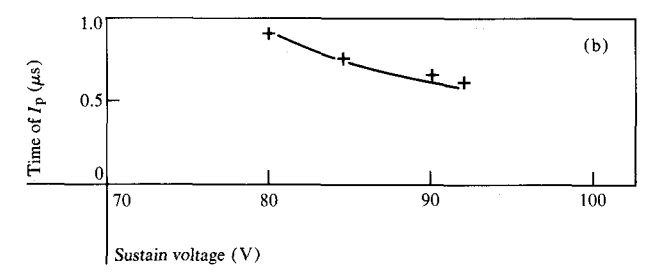


Figure 6 (a) Computed and measured values of the quantity of charge transferred each firing and the magnitude of the current peak, each as a function of the magnitude of applied sustain voltage. (b) Delay of the current peak for experimental and calculated results.

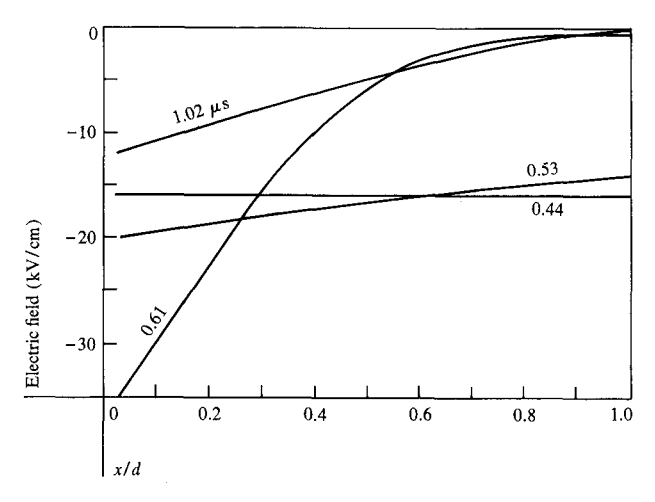


Figure 7 Computed electric field intensity as a function of position and time.

with a value of 800 pF cm⁻², which is in good agreement with experimental results [23].

Results

The results of the calculations are shown in the following figures and, where applicable, compared with experimen-

tal results. Figure 4 shows the applied voltage, $V_{\rm a}$, the voltage dropped across the gas, $V_{\rm g}$, and the current, i, each as a function of time for a mid-sustain voltage of 85 V. Note that the current occurs as a narrow spike each half cycle of sustain voltage, and the peak is delayed slightly from the start of the cycle. The voltage across the capacitor at any time is $V_{\rm a}-V_{\rm g}$.

Figure 5 shows a comparison of the experimentally determined [24] "voltage transfer curve" with the values computed by a model in the stable mode of operation. The experimental curve represents a plot of $(\Delta V_{...})$, the total voltage transferred to the wall capacitor during a half cycle as a function of the sum of V_a and V_{co} , where V_{co} represents the capacitor voltage at the start of the cycle. The maximum amplitude of sustain voltage for bistable operation is calculated by assuming V_{co} to be zero; then V_a is increased in small steps until the cell shows a distinct tendency to ignite, as evidenced by a progressive growth in the initial wall voltage, $V_{\rm co}$, of succeeding half cycles. The lower voltage limit for bistable operation is obtained next by progressively reducing V_a in small steps from this maximum sustain voltage, assuming V_{co} equal to V_a , and finding a minimum sustain voltage for which the cell shows a distinct tendency to approach [25] a steady state in successive cycles. Note that the computed range of bistable operation is also in good agreement with the experimental results.

Figure 6(a) shows the computed and measured values of the quantity of charge transferred each firing and the magnitude of the current peak, each as a function of the magnitude of applied sustain voltage. Figure 6(b) compares the delay of the current peak for experimental and calculated results.

Figure 7 shows the computed electric field intensity as a function of position and time for a mid-sustain voltage of 85 V. The maximum distortion occurs at about the same time as the current peak. The distortion of the field accentuates the effect of electronic back-scattering by greatly increasing the electric field at the cathode.

Figure 8 shows the computed variation in density of each of the charged particles and metastable atoms as a function of time, for a position in the gap 75 percent of the way to the anode, and for a mid-sustain voltage of 85 V. Note that after about 2 μ s, a plasma consisting of A^+ and electrons exists at this part of the gap. The decay of neon metastables results in a generation of A^+ via the Penning effect, which is of prime importance in these discharges. Atomic neon ions are seen to dominate in the active discharge period and then as the gas voltage falls they diminish progressively and convert to molecular neon ions. The presence of a significant density of charge particles from the previous firing provides starting charges for each new firing. Although not shown, the flux of the various active species hitting the cathode shows the same qualitative

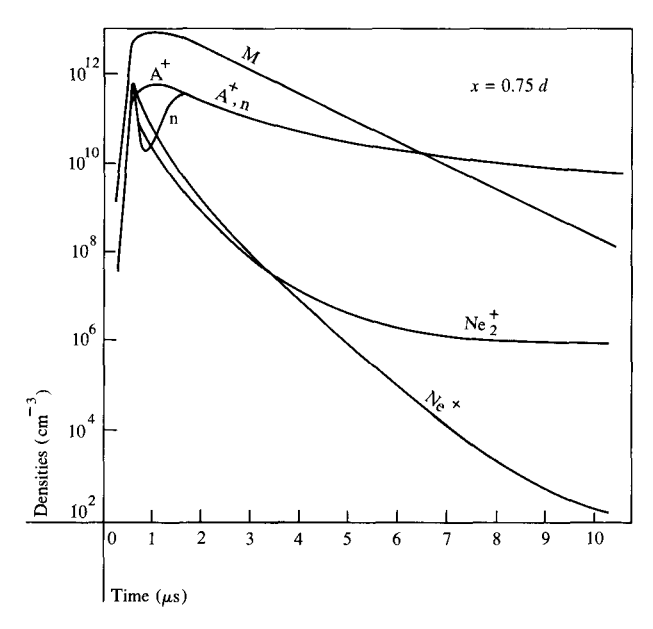


Figure 8 Computed variation in density of each of the charged particles and metastable atoms as a function of time, for a position in the gap 75% of the way to the anode.

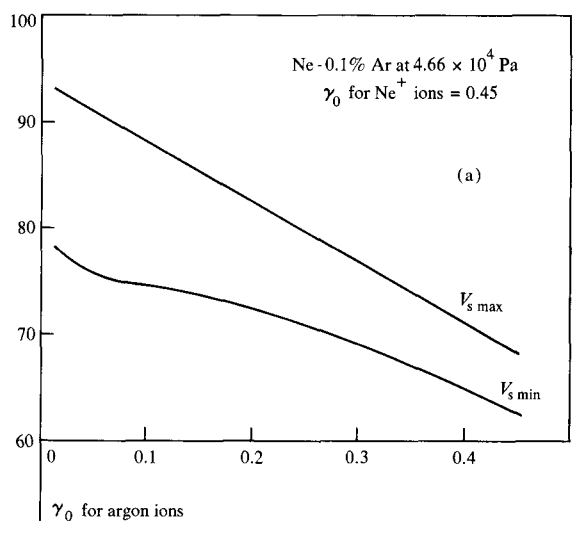
pattern—the flux of atomic neon ions predominates in the initial period of active discharge activity, but by about 1 μ s the flux of argon ions assumes a dominant position which continues for the rest of the period. The diffusive flux of neon metastables is well below the electric field driven ionic fluxes.

Finally, the theoretical model has been used to predict the variation of the operating voltage margin with respect to the intrinsic secondary-electron emission coefficients for MgO bombarded by both argon [Fig. 9(a)] and neon [Fig. 9(b)] ions. All the rest of the parameters were kept the same as for Figs. 4–8. In particular, we assumed the average speed of the emitted electrons to be independent of the variation of the γ_0 for both the neon and the argon ions. The strong dependence shown in these curves of the bistable margins versus secondary emission coefficient is probably responsible for the extreme susceptibility of this device to the preparation and subsequent treatment of the topcoat surface.

In conclusion, the present model shows all the qualitative features associated with plasma panels. Quantitative agreement with experimental data is reasonably good, which inspires confidence in the general validity of the method.

Acknowledgments

The authors are grateful to E. S. Schlig and G. R. Stilwell, Jr. for providing the experimental data used in this paper for comparison with theoretical calculations. Numerous discussions with W. E. Howard were extremely beneficial throughout the course of this work.



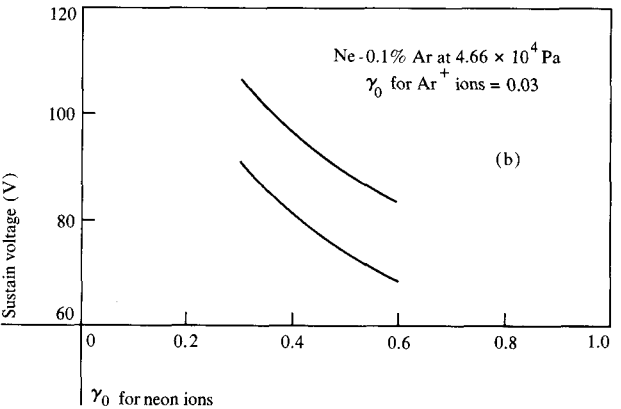


Figure 9 (a) Computed variation of the maximum and minimum sustain voltages as a function of the intrinsic secondary emission coefficient for argon ions. (b) Computed variation of the maximum and minimum sustain voltages as a function of the intrinsic secondary emission coefficient for neon ions.

References and note

- R. N. Jackson and K. E. Johnson, "Gas Discharge Displays: A Critical Review," Advances in Electronics and Electron Physics, vol. 35, L. Marton, ed., Academic Press, Inc., New York, 1974, pp. 191-267.
- H. Vernon and C. C. Wang, "AC Electrical Breakdown of Neon with External Electrodes," J. Appl. Phys. 43, 2664 (1972).
- 3. C. Lanza, "Analysis of an AC Gas Display Panel," *IBM J. Res. Develop.* 18, 232 (1974).
- F. M. Lay, C. K. Chu, and P. H. Haberland, "Simulation of Cyclic Operation of a Gas Panel Device," *IBM J. Res. Develop.* 18, 244 (1974).
- L. F. Weber, "Discharge Physics Studies for the AC Plasma Display Panel," Conf. Record, 1974 Biennial Display Devices and Systems (IEEE, 1974), pp. 20-26.
- L. F. Weber, "Discharge Dynamics of the AC Plasma Display Panel," Coordinated Sci. Lab. Report R-687, University of Illinois, Urbana, IL, Aug. 1975.
- O. Sahni and C. Lanza, "Origin of the Bistable Voltage Margin in the AC Plasma Display Panel," *IEEE Trans. Electron Devices* ED-24, 853 (1977).

- A. A. Kruithof and F. M. Penning, "Determination of the Townsend Ionization Coefficient α for Mixtures of Neon and Argon," *Physica (Utr.)* 4, 630 (1937).
- F. M. Lay and C. K. Chu, "Simulation of a Transient DC Breakdown in a Penning Mixture Between Two Closely Spaced Parallel Electrodes," J. Appl. Phys. 44, 4008 (1973).
 W. P. West, T. B. Cook, F. B. Dunning, R. D. Rundel, and
- W. P. West, T. B. Cook, F. B. Dunning, R. D. Rundel, and R. F. Stebbings, "Chemiionization Involving Rare Gas Metastable Atoms," J. Chem. Phys. 63, 1237 (1975).
- H. S. W. Massey, E. H. S. Burhop, and H. B. Gilbody, Electronic and Ionic Impact Phenomena, vol. III, Clarendon Press, Oxford, England, 1971, pp. 1801–1806.
- A. V. Phelps, "Diffusion, De-excitation, and Three-Body Collision Coefficients for Excited Neon Atoms," Phys. Rev. 114, 1011 (1959).
- A. P. Vitols and H. J. Oskam, "Reaction Rate Constant for Ne⁺ + 2 Ne → Ne⁺₂ + Ne," Phys. Rev. A 5, 2618 (1972).
 D. K. Bohme, N. G. Adams, M. Mosesman, D. B. Dunkin,
- D. K. Bohme, N. G. Adams, M. Mosesman, D. B. Dunkin, and E. E. Ferguson, "Flowing Afterglow Studies of the Reactions of the Rare-Gas Molecular Ions He⁺₂, Ne⁺₂, and Ar⁺₂ with Molecules and Rare-Gas Atoms," J. Chem. Phys. 52, 5094 (1970).
- H. J. Oskam and V. R. Mittelstadt, "Recombination Coefficient of Molecular Rare-Gas Ions," Phys. Rev. 132, 1665 (1963).
- O. Sahni and C. Lanza, "Importance of the Dependence of the Secondary Electron Emission Coefficient on E/P for Paschen Breakdown Curves in AC Plasma Panels," J. Appl. Phys. 47, 1337 (1976).
- O. Sahni and C. Lanza, "Influence of the Secondary Electron Emission Coefficient of Argon on Paschen Breakdown Curves in AC Plasma Panels for Neon + 0.1% Argon Mixture," J. Appl. Phys. 47, 5107 (1976).

- C. Lanza, W. E. Howard, and O. Sahni, "Numerical Simulation of AC Gas Display Discharges," Bull. Amer. Phys. Soc. Series II 20, B 255 (1975); also, J. Appl. Phys. 49, 2365 (1978).
- J. K. Theobald, "Investigation of Back Diffusion of Photoelectrons in Various Standard Gases as It Affects Secondary Electron Emission Coefficients," J. Appl. Phys. 24, 123 (1953).
- H. J. Oskam and V. R. Mittelstadt, "Ion Mobilities in Helium, Neon, and Argon," Phys. Rev. 132, 1435 (1963).
- J. M. Anderson, "Hall Effect and Electron Drift Velocities in the Plasma of the Positive Column," Phys. Fluids 7, 1517 (1964).
- N. J. Chou, "Ion-induced Secondary-Electron Emission from MgO Films," J. Vac. Sci. Technol. 14, 307 (1977).
- E. S. Schlig and G. R. Stilwell, Jr., IBM J. Res. Develop. 22, 634 (1978, this issue).
- 24. E. S. Schlig and G. R. Stilwell, Jr., private communication.
- 25. The steady ON state in the vicinity of the minimum sustain voltage was not precisely determined since the computation time becomes excessively long for the large number of successive cycles required to reach a stable point in this voltage region of operation.

Received March 25, 1977; revised October 3, 1977

The authors are located at the IBM Thomas J. Watson Research Center, Yorktown Heights, New York 10598.